Journal of Solid State Chemistry **154,** 61–67 (2000)
doi:10.1006/jssc.2000.8812, available online at http://www.idealibrary.com on IDEAL®

Structural Defects of Some Icosahedral Boron-Rich Solids and Their Correlation with the Electronic Properties

R. Schmechel[1] and H. Werheit

Solid State Physics Laboratory, Gerhard-Mercator University of Duisburg, D-47048 Duisburg, Germany

Received September 9, 1999; accepted January 2, 2000

For β-rhombohedral boron and boron carbide, the hitherto best-investigated icoasahedral boron-rich solids, the concentrations of structural defects and electronic gap states are quantitatively correlated. In this way the theoretically determined valence electron deficiencies are exactly compensated, and the metallic character of these solids resulting in the theoretical calculations on hypothetical idealized structures is changed to the experimentally proved semiconducting behavior. Obviously, the structural defects in these crystals are the necessary consequence of the valence electron deficiency. It is suggested that this correlation holds for icosahedral boron-rich solids in general. © 2000 Academic Press

1. INTRODUCTION

Careful fine-structure investigations of numerous crystalline boron-rich solids indicate that apart from α-rhombohedral boron, whose structure is formed by one B_{12} icosahedron on the vertex of the rhombohedral unit cell, the structures exhibit considerable concentrations of structural defects in the form of vacancies and antisite defects. At least in many cases, insufficient preparation methods can be excluded as the reason. This suggests that they are fundamental peculiarities of those structures.

For α-rhombohedral boron, β-rhombohedral boron, boron carbide, and YB_{66}, which are discussed below in some detail, the intrinsic structural defects and their concentrations result from the occupation densities determined by X-ray fine structure investigations:

- In α-rhombohedral boron the two different atomic sites B(1) and B(2) are completely occupied, and hence the defect concentration is zero.
- In β-rhombohedral boron the regular B(13) position is 74.5(6)% occupied (1) and sites B(16)–B(20) are 27.2, 8.5, 6.6, 6.8 and 3.7% occupied (in total 1.7 B atoms per unit cell) respectively (2, 3). This leads to an intrinsic point defect density of about 4.9 defects per unit cell (~ 4.7 at.%).
- In boron carbide the variation of carbon content within the homogeneity range can be taken as a specific kind of defect because the substitution takes place on regular sites in the structure (4–9) In detail, the concentrations of B_{12} and $B_{11}C$ icosahedra and CBB and CBC chains vary and chainless unit cells occur, when the composition is shifted from the carbon-rich limit $B_{4.3}C$ of the homogeneity range to more boron-rich compositions (10, 11). According to Bylander *et al.* (12) $B_{13}C_2$ [structure formula B_{12}(CBC)] is the energetically most favorable structure. If this is taken as a reference, based on the 42% B_{12} icosahedra, 58% $B_{11}C$ icosahedra, 62% CBC chains, 20% CBB chains, and ~ 19% missing chains experimentally determined by Kuhlmann *et al.* from phonon spectroscopy (10, 11), the defect concentration in $B_{13}C_2$ is ~ 9.3 at.%.
- According to Higashi *et al.* (13) the occupancies of sites B(10)–B(13) in the nonicosahedral B_{80} unit of YB_{66} are 72, 65, 31, and 22%, respectively, leading to an actual number of ~ 42 B atoms in this B_{80} unit and to an average defect concentration of ~ 17 at.% of the whole structure.

The experimentally determined electronic properties of these complex boron structures doubtlessly characterize them as semiconductors; their properties, however, qualitatively deviate from those of classic semiconductors. They exhibit largely common peculiarities like semiconducting behavior despite the odd number of valence electrons per unit cell, hopping conduction even in high-purity crystals, *p*-type conduction, which is difficult to overcompensate to *n*-type. Obviously, one essential reason for this relationship of electronic properties is the icosahedra as common structural elements.

Franz and Werheit (14, 15) pointed out the role of Jahn–Teller distortion of the B_{12} icosahedra leading to separation of occupied and unoccupied electronic states, thus explaining the semiconducting behavior. They attributed the experimentally proved electronic level 190 meV above the actual valence band (16) in β-rhombohedral

[1] Present address: Darmstadt University of Technology, Material Science, Department of Electronic Materials, D-64287 Darmstadt, Germany.

0022-4596/00 $35.00
Copyright © 2000 by Academic Press
All rights of reproduction in any form reserved.

boron to a Jahn–Teller splitting of valence states. However, there remained the inconsistency that the optical interband transitions seemed to indicate band-type behavior of this split-off band implying extended states, while the interpretation of the transport properties required localized states in this electronic level (17). Since the static Jahn–Teller effect distorts the B_{12} icosahedra of the structure in the same way, the resulting electronic states have the translation symmetry of the crystal and should be delocalized.

The configuration interaction (CI) calculation by Fujimori and Kimura (18) on the icosahedral $B_{12}H_{12}$ cluster, well representing the bonding of B_{12} icosahedra in β-rhombohedral boron and boron carbide, proved that the Jahn–Teller effect distorting the regular icosahedron to the D_{3d} symmetry of the α- and β-rhombohedral boron structure groups leads to a separation between ground and first excited states of about 1.5 eV. This value is close to the typical bandgaps of many icosahedral boron-rich solids, which seem to be accordingly explained; however, it considerably exceeds the distance between the actual valence band and the split-off band. Hence its attribution to the Jahn–Teller effect cannot be maintained and its identification requires new considerations.

Electronic band structure calculations have only become available for α-rhombohedral boron (19–23), β-rhombohedral boron (24), and boron carbide (B_4C and $B_{13}C_2$) (12, 25–27). They are based on idealized structures without defects but use the real atomic positions known from fine-structure investigations, and thus the Jahn–Teller distortion of the B_{12} icosahedra can be assumed to be implicitly considered. While the band structures calculated by different authors differ slightly in energies and symmetry properties, the densities of valence states are largely consistent and, apart from α-rhombohedral boron, deficiencies of valence electrons result (~ 1.5% for β-rhombohedral boron and ~ 2% for boron carbide $B_{13}C_2$). Compensation of these deficiencies by structural defects is suggested in (12, 24), and Bullet (28) assumes that the numerous intrinsic defects in the structure could have an electronic origin. However, these aspects have not yet been discussed in detail. The experimentally proven high densities of electronic states in the bandgaps of the icosahedral boron-rich solids are missing in all calculated band structures.

The calculated deficiencies of electrons in the valence bands and the concentrations of structural defects are compared for some structures in Table 1. Obviously, there is a strong correlation, suggesting the valence electron deficiency to be the driving force for the generation of structural defects in icosahedral boron-rich solids.

2. ELECTRONIC PROPERTIES OF POINT DEFECTS

Since theoretical calculations on the electronic properties of point defects in icosahedral boron-rich solids are missing, the different kinds of point defects and their effect on the electronic structure are qualitatively considered:

The electronic states of interstitial atoms are localized due to the lack of translation symmetry. Hence the number of valence band states remains unchanged, while the number of valence electrons increases, when the interstitial atom is ionized.

In a covalent crystal every regular bond between neighboring atoms contributes to the total number of valence band states. In a vacancy these regular bonds are broken.

TABLE 1
Calculated Electron Deficiencies for the Valence Bands of Idealized Crystal Structures and Experimentally Determined Point Defect Concentrations in the Real Crystals

Idealized crystal structure				Real crystal structure		
Valence states (per unit cell)	Valence electrons [(unit cell)$^{-1}$]	Electron deficiency [(unit cell)$^{-1}$]	Electronic character (theorectical)	Electronic character (experimental)	Intinsic point defects (per unit cell)	
α-Rhombohedral boron						
36[a]	36	0	Semicond.	Semicond.	0[b]	
β-Rhombohedral boron						
320[c]	315	5	Metal	Semicond.	4.92(20)[d]	
Boron carbide						
$B_{13}C_2$ [idealized structure formula B_{12}(CBC)]						
48[e]	47	1	Metal	Semicond.	0.97(5)[f]	
$B_{4.3}C$ [idealized structure formula: $B_{11}C$ (CBC)]						
48[e]	47,83	0,17	Metal	Semicond.	0.19(1)[f]	
Hypothetical B_4C [idealized structure formula: $B_{11}C$ (CBC)]						
48[e]	48	0	Semicond.	—	—	—

[a] Reference (19). [b] Reference (4). [c] Reference (24). [d] Reference (2). [e] Reference (25). [f] References (10, 11).

The reconstructed bonds have no translation symmetry and hence the related unoccupied electronic states are localized and energetically separated from the valence band. Accordingly, vacancies reduce the number of valence band states.

In the binary compound boron carbide antisite defects occur, when C substitutes for B or vice versa. Since the number of electrons of the atoms differs by only one, an antisite defect generates a donor site and an acceptor state. The acceptor removes one electron from the lattice and reduces the number of valence band states by one. This occurs as an unoccupied localized state, which is shifted into the bandgap. The donor provides an additional electron, but it does not change the number of valence band states.

Based on these considerations, the number of electronic states that are generated by the above-mentioned structural defects can be estimated as follows.

2.1. *β-Rhombohedral Boron*

There are 1.52 vacancies in the rhombohedral unit cell [6 partially occupied crystallographically equivalent B(13) sites] and 3.38 interstitial atoms [weakly occupied sites B(16)–B(20)]. Bullet (24) calculated for an idealized structure [sites B(1)–B(15) fully occupied, B(16)–B(20) unoccupied] 320 valence band states occupied by $3 \times 105 = 315$ valence electrons.

The B(13) site has the coordination number 6 like the surrounding B sites, and hence one-half of the 3 valence electrons can be attributed to each regular bond. For each B(13) vacancy 3 electronic states and 3 electrons are removed from the valence band. Moreover, $6 \times \frac{1}{2} = 3$ occupied localized electronic states from the surrounding B atoms additionally reduce the number of regular valence states by 3. In total, for each vacancy 6 electronic states and 6 electrons are removed from the valence band. However, the 3 electrons in the localized states may fall into the energetically more favorable unoccupied valence band states. Hence, from the 1.52 B(13) vacancies per unit cell $3 \times 1.52 = 4.56$ unoccupied localized states are generated, which are energetically separated from the valence band. Compared with the calculated deficiency of five valence electrons this would satisfactorily explain the semiconducting character of β-rhombohedral boron.

Additional electrons come from the interstitial B(16)–B(20) sites, leaving the number of valence states unchanged. Accordingly, there are $3 \times 1.52 + 3 \times 3.38 = 14.70$ electrons per unit cell available compared with the valence electron deficiency of 5. Assigning an error of only 2% to the occupation densities obtained from the literature, the completely occupied valence band leaves 10 electrons per unit cell for the occupation of localized gap states originating from the B(13) vacancies or from interstitial B(16)–B(20) states. If one assumes that the B(13) vacancy generates a gap state, which can be occupied by two paired electrons, similar to the vacancy V^{2+} state in silicon (29, 30) the number of interstitial B(16)–B(20) atoms exactly corresponds to the number of unoccupied sites in this orbital. If single ionization of the interstitial B atoms is assumed, the valence band and the B(13) vacancy orbitals are exactly filled up.

That assumption easily explains the ESR results. The density of paramagnetic centers [about 10^{15} cm^{-3} (31)] is very low compared with the defect concentration (about 10^{20} cm^{-3}) and can be appreciably enhanced only by heating or optical excitation (32, 33). Moreover, it is consistent with the charge transport in β-rhombohedral boron preferably due to hopping processes but with a certain contribution of delocalized carriers [see (34)]. Hence it seems evident that the experimentally proved electronic level 0.19 eV above the actual valence band [see (34)] is formed by orbitals of the B(13) vacancy and occupied by paired localized electrons originating from the intrinsic structural defects.

This rough estimation demonstrates that the concentration of intrinsic structural defects in β-rhombohedral boron is able to exactly compensate the electron deficiency calculated for the valence band of the idealized structure. Indeed, further investigations, in particular on the molecular orbitals of the intrinsic defects in β-rhombohedral boron, are necessary to confirm this model.

2.2. *Boron Carbide*

The idealized, according to theoretical calculations (26, 27), energetically most favorable structure of boron carbide $B_{13}C_2$ [structure formula B_{12}(CBC)] is taken as reference to determine the concentration of structural defects. These are antisite defects like $B_{11}C$ icosahedra (donors) and CBB chains (acceptors) and vacancies in the unit cells without chains [alternatively α-rhombohedral boron like or B□B arrangements with two separated B atoms and vacant B(3) site based on phonon spectroscopy (10, 11), B□B arrangements according to the calculation of reaction kinetics (35), vacancy of B(3) without specification of the chain end atoms, derived from neutron scattering (6)]. Interstitial atoms in boron carbide are not known, except possibly for Al, which occupies sites sideways shifted from the main diagonal in chainless unit cells (36).

The valence band of boron carbide contains 48 electronic states per unit cell, while the number of valence electrons depends on the carbon content. For $B_{13}C_2$ 47 and for $B_{12}C_3$ [structure formula B_{11}C(CBC)] 48 valence electrons per unit cell are available (23).

In an antisite defect the C → B substitution is a donor and the B → C substitution an acceptor. For each pair the total number of valence electrons remains unchanged, but every acceptor state reduces the valence band states by one. To compensate the electron deficiency of one per unit cell by antisite defects, one acceptor state per unit cell is necessary. This would require complete transformation of the idealized structure B_{12}(CBC) to B_{11}C(CBB) in contrast to the real

TABLE 2

Calculated Concentrations of Structure Elements in Boron Carbide ($B_{13}C_2$) for Different Configurations of the 19% Chain-Free Unit Cell

	Concentration of structure elements			
	Assumed configuration (□ = vacancy)			
Structural element	C□C	B□B	□□□	Experimental
Chain-free cells (exp†)	19%	19%	19%	19%[a]
B_{12}-icosaedra	31%	42%	70%	42%[b]
$B_{11}C$-icosahedra	69%	58%	30%	58%[b]
CBC chains	9%	62%	81%	62%[b]
CBB chains	72%	19%	0%	19%[b]

[a]References (6, 10, 11)
[b]References (10, 11).

structure, which, however, contains vacancies in $\sim 19\%$ chainless unit cells (6, 10, 11) as further defects to compensate the valence electron deficiency.

In a first step the following chain configurations in the 19% chainless cells are assumed to be possible: C□C, B□B, □□□ (□, vacancy). The concentration of CBB chains is calculated according to the requirement to compensate the valence electron deficiency. Then the concentrations of B_{12} and $B_{11}C$ icosahedra result from the stoichiometry. In the C□C configuration, two electronic states around the vacancy become localized, reducing the number of states in the regular valence band. The remaining valence electron deficiency can be compensated by antisite defects $B \rightarrow C$. One vacancy and two antisite defects are attributed to the B□B configuration. In the □□□ configuration the structural defects would be sufficient to compensate the electron deficiency by six broken bonds at the chain ends reducing the valence band states by $6 \times 0.2 = 1.2$ per unit cell, but it is known from α-rhombohedral boron that this configuration is not very stable. The resulting concentrations of the different structure elements are compared in Table 2.

For the assumed B□B configuration the calculated concentrations of the structure elements agree with the results experimentally determined by Kuhlmann and Werheit (10, 11) and make this structure assumption the most probable. Accordingly, in the chain-free unit cells occupation of the end position of the chain by carbon atoms [alternative model in (10,11)] is definitely excluded.

With increasing carbon content the concentration of $B_{11}C$ icosahedra increases, with the carbon atoms acting as donors. The correspondingly increasing number of valence electrons reduces the probability of vacancies assumed to be formed to compensate the electron deficiency. Idealized B_4C has 48 valence electrons and should be able to form a crystal without vacancies. Indeed, $B_{4.3}C$ boron carbide at the experimentally determined carbon-rich limit of the homogeneity range (37, 38) was shown to have no chain-free unit cells (10, 11).

If the carbon content is lower than in $B_{13}C_2$, the electron deficiency increases, and additional vacancies generating acceptor states by transforming $B_{12}(CBC)$ to $B_{11}C(CBB)$ are expected. Accordingly, compared with $B_{13}C_2$ more $B_{11}C$ icosahedra should be formed in despite the lower carbon content, and the concentrations of CBB chains and chain-free unit cells should increase.

Based on this qualitative consideration the concentrations of the different elements of the boron carbide structure were calculated with the following assumptions:

i. The electron deficiency D is compensated by B□B and CBB generating 4 and 1 acceptor site, respectively. $D = 4c(\text{B□B}) + c(\text{CBB})$.

ii. The relation $R = c(\text{CBB})/c(\text{CBC})$ is taken from the oscillator strengths of the stretching mode of CBB and CBC chains, respectively [see Fig. 7 in (11)]. In this quotient the not excludable influence of experimental error in determining the absolute oscillator strengths of the chains is largely eliminated.

iii. Each rhombohedral unit cell has any arrangement on the main diagonal; accordingly $c(\text{B□B}) + c(\text{CBB}) + c(\text{CBC}) = 1$.

This leads to

$$c(\text{B□B}) = (R(D-1) + D)/(3R + 4).$$

After the concentrations of CBB and CBC chains are calculated, the numbers of B_{12} and $B_{11}C$ icosahedra immediately result from the stoichiometry. In Fig. 1 the

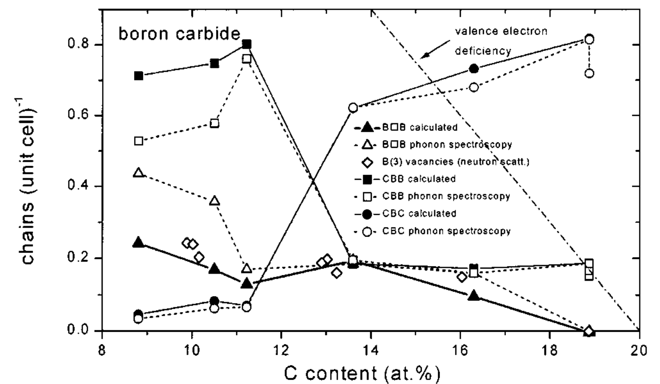

FIG. 1. Density of atom arrangements on the trigonal axis of the rhombohedral unit cell of boron carbide (CBC and CBB chains, B□B arrangements): solid symbols, this work; open symbols, determined by phonon spectroscopy (10, 11); diamonds, B(3) vacancies (center of the three-atom chain) determined by neutron scattering (6). The reason for the considerable difference close to the boron-rich limit of the homogeneity range is that in the phonon spectroscopy the absolute oscillator strengths were used, while in the present work their relation is taken and thus experimental error by light scattering at nonideal surfaces is largely eliminated. Calculated valence electron deficiency for comparison.

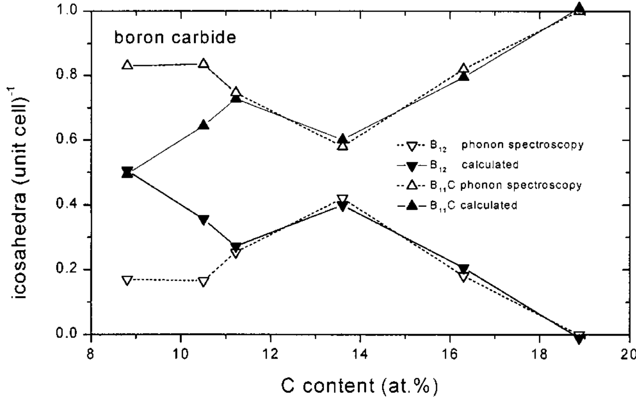

FIG. 2. Density of B_{12} and $B_{11}C$ icosahedra calculated from the densities of the atoms on the trigonal axis (Fig. 1) and the stoichiometry of the samples [for details see Table 1 in (11)]; solid symbols, this work; open symbols, determined by phonon spectroscopy (10, 11). For the differences close to the carbon-rich limit of the homogeneity range see Fig. 1.

accordingly calculated concentrations of the different structural elements are compared with those derived from phonon spectroscopy (10, 11) (recalculated for the B□B arrangement). Between about $B_{11}C$ and the carbon-rich limit of the homogeneity range $B_{4.3}C$ the agreement is excellent. Moreover the calculated B□B concentration is well confirmed by the B(3) vacancies determined by neutron scattering (6). The uncertainty of the quantity of B□B configurations close to the boron-rich limit of the homogeneity range is probably caused by the attribution of the CBB and CBC densities to the experimentally determined oscillator strength (10, 11) (Fig. 2). This could yield too small quantities because of the strong damping of the oscillators, which are therefore not clearly separated enough from the background absorption.

Recent investigations on isotope-enriched boron carbide (39) have shown that certain, not yet specified preparation conditions apparently allow the reproducible formation of small quantities of CCC chains in boron-rich boron carbides. This C → B substitution in the B(3) site is a possibility to generate donors alternatively to that by $B_{11}C$ icosahedra considered above. For the attribution of CCC arrangements to the separated chain phonon one obtains the following partly modified relations:

i. Since C on the central chain position of a CCC chain generates a donor and therefore has no influence on the valence band density of states, there the compensation of the valence electron deficiency $D = 4c(\text{B}\square\text{B}) + c(\text{CBB})$ remains the same like above.

ii. $R = c(\text{CBB})/c(\text{CBC})$ unchanged as well.

iii. The relation $R_2 = c(\text{CCC})/(c(\text{CBB}) + c(\text{CBC}))$ is taken from the phonon oscillator strengths of the accordingly attributed phonons [see (39)].

iv. Each rhombohedral unit cell has any arrangement on the main diagonal; accordingly, $c(\text{B}\square\text{B}) + c(\text{CBB}) + c(\text{CBC}) + c(\text{CCC}) = 1$.

For these assumptions one gets

$$c(\text{B}\square\text{B}) = \frac{D(1 + R_2)(R + 1) - R}{4(1 + R_2)(R + 1) - R}.$$

The accordingly calculated concentrations of the different atom arrangements on the main diagonal of the unit cell are displayed in Fig. 3 and the resulting concentrations of the icosahedra in Fig. 4. Because of the small share of CCC chains their influence on the concentrations of the other

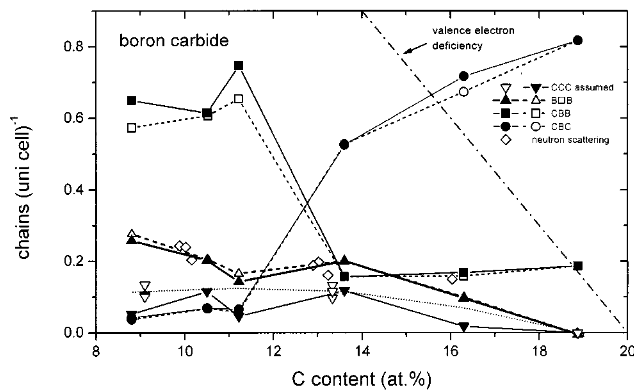

FIG. 3. Concentrations of CBC, CBB, CCC chains, and B□B arrangements on the trigonal axis per unit cell versus C content. Full lines connecting full symbols represent results based on the averaged CCC concentrations determined for the isotope-enriched samples (39). Dashed lines connecting open symbols represent results based on the measured oscillator strengths of the additional chain phonon obtained from (1, 2, 9); Diamonds represent B(3) vacancies determined by neutron scattering (6).

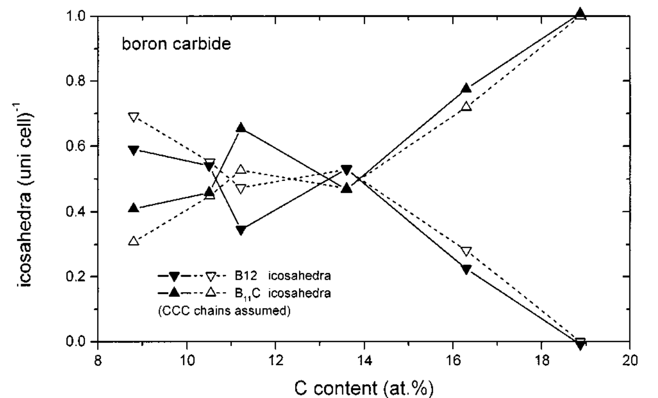

FIG. 4. Concentrations of B_{12} and $B_{11}C$ icosahedra versus C content. Full symbols, based on the averaged concentration of CCC chains (see Fig. 3); open symbols, based on the measured oscillator strengths of the additional chain phonon obtained from (10, 11) [see also (39)].

atom arrangements within the unit cell is small. However, the concentration of $B_{11}C$ icosahedra in the boron-rich range of the homogeneity range is remarkably reduced.

3. CONCLUSION

The results indicate that the idealized structures of icosahedral boron-rich solids, so far as they lead to valence electron deficiencies in theoretical band structure calculations, are energetically less favorable than structures with defects but completely filled valence bands. Those defects are responsible for high-density gap states, which essentially determine the electronic conductivity mechanism and numerous other physical properties in these semiconductors. It seems that the correlation between structural defects and electronic gap states is a general property of icosahedral boron-rich solids and is only missing when the electron deficiency is accidentally zero as in α-rhombohedral boron. This result strongly supports the concept that the basic electronic band structures of the icosahedral boron-rich solids are typical of crystals [see (34, 40) and references therein], and disproves Golikova's "amorphous concept" [see (41) and references therein], which assumes that the localized states come from an amorphization depending on the number of atoms in the unit cell. As shown, in reality the localized states are generated by well-defined structural defects and are required to compensate the electron deficiency of the related idealized structure.

These localized states form in β-rhombohedral boron the electronic levels ∼ 190 meV above the valence band edge, which is responsible for the hopping processes prevailing in the electronic transport. The usually small share of nonlocalized holes is generated by the thermal activation of electrons from the valence band into this level [see (34) and references therein]. The mentioned inconsistency of the optical interband absorption attributed to indirect allowed transitions from this level (16) was solved by the attribution to nondirect transitions, which have the same dependence on photon energy and a very similar temperature dependence (42).

At the carbon-rich limit of the homogeneity range of boron carbide, the ∼ 17% concentration of CBB chains coincides exactly with the electron deficiency. That CBB concentration is largely independent of the C content down to about 13.5% and therefore obviously intrinsic. This explains why $B_{4.3}C$ is indeed the limit of the homogeneity range (37, 38). Assuming that the CBB chains are thermally generated at the temperature of preparation, the temperatures of melting T_m ∼ 2750 K and hot-pressing T_{hp} ∼ 2300–2400 K yield activation energies of 0.42 and 0.36 eV, respectively, which are of the order of magnitude for point defects. This suggests that boron carbide with a higher content of bonded carbon than in $B_{4.3}C$ can be obtained only if a chemical reaction of the elements is possible at low temperatures; e.g., for magnesiothermal boron carbide (reaction temperature ∼ 2000 K) a CBB content of 8–10% and accordingly the most carbon-rich composition $B_{4.15}C$ are expected.

The maximum electrical conductivity of boron carbide occurs at about 13.5% C, where the concentration of B_{12} icosahedra is maximum and that of $B_{11}C$ is minimum [see (43) and references therein]. This contradiction to the hole bipolaron hypothesis, which attributes the electrical conductivity to hole bipolaron hopping between $B_{11}C$ icosahedra (44–47), is unequivocally substantiated by the results in the present paper. Figure 5 shows that the density of states determined from the electrical conductivity [see (43)] is inversely correlated with the total density of point defects ($B_{11}C$ icosahedra, CBB chains, and B□B arrangements).

The defect concentration in the YB_{66}-type crystals of about 17% exceeds that in the other icosahedral boron-rich solids by far. There are at least four well-defined defect sites leading to a corresponding variety of electronic levels in the band gap. This easily explains that the low-energy tail of the optical absorption edge (48, 49) is much stronger than for the other boron-rich solids.

For some other structure groups of icosahedral boron-rich solids the existence of defects has already been proven as well: (i) in the α-tetragonal structure group [idealized structure formula $(B_{12})_4X_2Y_2$] missing or incomplete occupations of the X, Y sites (50); (ii) in the β-tetragonal structure group [idealized structure formula $(B_{21}\cdot 2B_{12})_4(X_mY_n)$ missing or incomplete occupations of X, Y sites, two B vacancies in B_{21} double icosahedra (B_{19} in α-AlB_{12}) (50); (iii) in the orthorhombic $MgAlB_{14}$-type compounds [idealized structure formula $(B_{12})_4Me(1)_4Me(2)_4B_8$] incomplete occupations of the $Me(1)$ and $Me(2)$ sites, possibly incomplete occupation of the nonicosahedral B sites [see (51) and

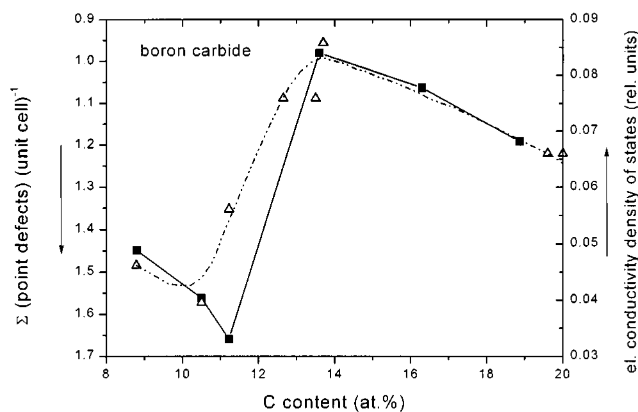

FIG. 5. Total density of point defects ($B_{11}C$ icosahedra, CBC, CBB, B□B) (this work) compared with the density of states derived from the electrical conductivity using Mott's law for variable-range hopping [see (43) and references therein] versus carbon content.

references therein]. Unfortunately, for these structure groups the available band structure calculations and experimental studies of the electronic properties are not yet sufficient to check the correlation between defects and electronic properties. However, it seems obvious to assume that this correlation is a general property of icosahedral boron-rich solids.

REFERENCES

1. B. Calmer, *Acta Crystallogr.* **33,** 1951 (1977).
2. G. A. Slack, J. H. Rosolowski, C. Hejna, M. Garbauskas, and J. S. Kasper, *in* "Proc. 9th Int. Symp. Boron, Borides and Rel. Compd., Duisburg, Germany, Sept. 21–25, 1987" (H. Werheit, Ed.), p. 132.
3. G. A. Slack, C. J. Hejna, M. F. Garbauskas, and J. S. Kasper, *J. Solid State Chem.* **28,** 489 (1988).
4. B. Morosin, A. W. Mullendore, D. Emin, and G. A. Slack, *in* "Boron-Rich Solids" (AIP Conf. Proc. 140), (D. Emin, T. L. Aselage, C. L. Beckel, and I. A. Howard, (Eds.), p. 70. Am. Inst. of Physics, New York, 1986.
5. T. Lundström, *AIP Conf. Proc.* **231,** 186 (1991).
6. G. H. Kwei and B. Morosin, *J. Phys. Chem.* **100,** 8031 (1996).
7. H. Werheit, U. Kuhlmann, M. Laux, and R. Telle, *J. Alloys Compd.* **209,** 181 (1994).
8. H. Werheit, U. Kuhlmann, M. Laux, and R. Telle, *in* "Proc. 11th Int. Symp. Boron, Borides and Related Compounds, Tsukuba, Japan, August 22–26, 1993" (Jpn. J. Appl. Phys. Series 10) (R. Uno and I. Higashi, Eds.), p. 86.
9. H. Werheit, U. Kuhlmann, K. Shirai, and Y. Kumashiro, *J. Alloys Compd.* **233,** 121 (1996).
10. U. Kuhlmann and H. Werheit, *Solid State Commun.* **83,** 849 (1992).
11. U. Kuhlmann, H. Werheit, and K. A. Schwetz, *J. Alloys Compd.* **189,** 249 (1992).
12. D. M. Bylander, L. Kleinman, and S. Lee, *Phys. Rev. B* **42,** 1394 (1990).
13. I. Higashi, K. Kobayashi, T. Tanaka, and Y. Ishizawa, *J. Solid State Chem.* **133,** 16 (1997) (Proc. 12th ISBB'96, Baden, Austria, 1996).
14. R. Franz and H. Werheit, *Europhys. Lett.* **9,** 145 (1989).
15. R. Franz and H. Werheit, *AIP Conf. Proc.* **231,** 29 (1991).
16. H. Werheit, M. Laux, and U. Kuhlmann, *Phys. Status Solidi.* **176,** 415 (1993).
17. H. Werheit and F. Kummer, *J. Phys. Condens. Matter* **7,** 7851 (1995).
18. M. Fujimori and K. Kimura, *J. Solid State Chem.* **133,** 178 (1997) (Proc. 12th ISBB'96, Baden, Austria, 1996).
19. F. Perrot, *Phys. Rev. B* **23,** 2004 (1981).
20. D. W. Bullett, *J. Phys. C* **15,** 415 (1982).
21. H. Schöttke, *J. Less-Common Met.* **91,** 159 (1983).
22. D. R. Armstrong, J. Bolland, and P. G. Perkins, *Theor. Chi. Acta* **64,** 501 (1984).
23. S. Lee, D. M. Bylander, and L. Kleinman, *Phys. Rev. B* **42,** 1316 (1990).
24. D. W. Bullett, *J. Phys. C* **15,** 415 (1982).
25. D. R. Armstrong, J. Bolland, P. G. Perkins, G. Will, and A. Kirfel, *Acta Crystallogr. Sect. B* **39,** 324 (1983).
26. D. M. Bylander and L. Kleinman, *Phys. Rev. B* **43,** 1487 (1991).
27. L. Kleinman, *AIP Conf. Proc.* **231,** 13 (1991).
28. D. W. Bullett, *AIP Conf. Proc.* **231,** 21 (1991).
29. G. D. Watkins, *in* "Deep Centers in Semiconductors" (S. T. Pantelides, Ed.), p. 147. Gordon Breach, New York, 1986.
30. G. D. Watkins, *in* "Materials Science and Technology," Vol. 4: "Electronic Structure and Properties of Semiconductors" (W. Schröter, Ed.), p. 105. VCH, Weinheim, 1991.
31. C. D. Siems, *J. Less-Common Met.* **67,** 155 (1979).
32. D. Geist, *Z. Naturforsch. A* **28,** 953 (1973).
33. A. Nadolny, *Phys. Status Solidi B* **65,** 801 (1974).
34. H. Werheit, *in* "Landolt–Börnstein, Numerical Data and Fundamental Relationships in Science and Technology" (O. Madelung, Ed.), Group III, Vol. 41C, Ed. O. Madelung, p. 3. Springer, Berlin, 1998.
35. B. Kasper, MPI Stuttgart, personal communication (1996).
36. R. Schmechel, H. Werheit, K. Robberding, T. Lundström, and H. Bolmgren, *J. Solid State Chem.* **133,** 254 (1997).
37. K. A. Schwetz and P. Karduck, *AIP Conf. Proc.* **231,** 405 (1991).
38. K. A. Schwetz and P. Karduck, *J. Less-Common Met.* **175,** 1 (1995).
39. H. Werheit, T. Au, R. Schmechel, S. O. Shalamberidze, G. I. Kalandadze, and A. M. Eristav, *J. Solid State Chem.* **154**.
40. H. Werheit, *in* "Materials Science of Carbides, Nitrides and Borides" (Y. G. Gogotsi and R. A. Andrievski, Eds.), p. 65. Kluwer, Dordrecht, 1999.
41. O. A. Golikova, *AIP Conf. Proc.* **231,** 108 (1991).
42. R. Schmechel and H. Werrheit, *J. Solid State Chem.* **154**.
43. R. Schmechel and H. Werheit, *J. Solid State Chem.* **133,** 335 (1997).
44. I. A. Howard, C. L. Beckel, and D. Emin, *Phys. Rev. B* **35,** 2929 (1987).
45. I. A. Howard, C. L. Beckel, and D. Emin, *Phys. Rev. B* **35,** 9265 (1987).
46. D. Emin, *AIP Conf Proc.* **231,** 65 (1991).
47. D. Emin, *Phys. Rev. B* **48,** 691 (1993).
48. H. Werheit, U. Kuhlmann, and T. Tanaka, *AIP Conf. Proc.* **231,** 125 (1991).
49. U. Kuhlmann, H. Werheit, J. Hassdenteufel, and T. Tanaka, *in* "Proc. 11th Int. Symp. Boron, Borides and Related Compounds, Tsukuba, Japan, August 22–26, 1993" (Jpn. J. Appl. Phys. Series 10), p. 82, 1994.
50. I. Higashi, *AIP Conf. Proc.* **140,** 1 (1986).
51. H. Werheit, U. Kuhlmann, G. Krach, I. Higashi, T. Lundström, and Y. Yu, *J. Alloys Comd.* **202,** 269 (1993).